



The relationship between AGR2 levels and intestinal barrier function in high-fat diet animal models

Facai Kang¹, Shuhong Zhao^{1*}, Huimin Ren², Jing Yang³, Sizhen Chen¹, Qi Kou¹, Jing Sun^{4*}

¹ Department of Gastroenterology, Zhoushan Branch Ruijin Hospital, Shanghai Jiaotong University School of Medicine, Zhoushan, 316000, China

² Department of Gynaecology, Zhoushan Branch Ruijin Hospital, Shanghai Jiaotong University School of Medicine, Zhoushan, 316000, China

³ Department of Infection and Liver Disease, Zhoushan Branch Ruijin Hospital, Shanghai Jiaotong University School of Medicine, Zhoushan, 316000, China

⁴ Department of Gastroenterology, Rui Jin Hospital Affiliated to Shanghai Jiao Tong University School of Medicine, Shang Hai, 200025, China

ARTICLE INFO

Original paper

Article history:

Received: April 01, 2023

Accepted: December 22, 2023

Published: December 31, 2023

Keywords:

Animal models, antioxidant protein 2, high-fat diet, intestinal barrier function, inflammation

ABSTRACT

This study aimed to observe the effect of anterior gradient protein 2 (AGR2) levels on intestinal barrier function in HFD animal models. For this purpose, thirty healthy male clean-grade C57BL/6 mice were randomly separated into a normal control group and a high-fat group. The normal control group was fed a normal diet, while the high-fat group was fed an HFD for a total of 8 weeks. It collected body weight changes before and after modeling of two groups of rats and serum samples and detected fasting blood glucose, total cholesterol, triglycerides, AGR2, and diamine oxidase (DAO) concentrations. It collected the expression levels of AGR2 in the colon of rats after modeling, evaluated the permeability of the colon and small intestine barrier by Ussing chamber and Evan's blue (EB) methods, and analyzed the correlation between AGR2 levels and intestinal barrier function using Pearson correlation. Results showed that when the two groups of mice were fed for 8 weeks, their body weight, fasting blood glucose, total cholesterol, and triglycerides all met the characteristics of an HFD mouse model, and the model was successfully established. When the two groups of mice were fed for 8 weeks, the serum AGR2 concentration, relative expression of AGR2 in colon tissue, Gt, and EB content of the high-fat group mice were higher than those of the normal control group, and the difference was significant ($P < 0.05$); Meanwhile, the serum DAO concentration and Isc of the high-fat group mice were lower than those of the normal control group, with statistically significant differences ($P < 0.05$); The relative expression levels of serum AGR2 and colon AGR2 were negatively correlated with Isc ($r = -0.503, -0.623, P < 0.05$), and positively correlated with Gt ($r = 0.461, 0.560, P < 0.05$). There was a homogeneous distribution characteristic between the relative expression levels of serum AGR2 and serum DAO, colon AGR2, and Isc variables. It was concluded that HFD could upregulate the expression of AGR2 in mice, downregulate the level of DAO, and damage the intestinal barrier function of mice. Both serum AGR2 concentration and colonic AGR2 relative expression can participate in the regulation of colonic intestinal barrier function and can serve as potential indicators for evaluating intestinal barrier damage.

Doi: <http://dx.doi.org/10.14715/cmb/2023.69.15.20>

Copyright: © 2023 by the C.M.B. Association. All rights reserved.

Introduction

High-fat diet (HFD) is one of the important pathogenic factors for intestinal barrier dysfunction. Antioxidant protein 2 (AGR2) is a glandular secreted protein widely expressed in the intestine and closely related to the intestinal barrier (IB). However, the effect of AGR2 on the increase in IB permeability caused by HFD is not yet clear. Studies have shown that HFD can cause denaturation of the small intestinal tight junction protein inhaling, increasing intestinal permeability (1,2). AGR2 has a great influence on maintaining intestinal homeostasis in patients with ulcerative colon cancer and is crucial for maintaining the integrity of the IB. Based on this, it speculates that AGR2 may be involved in regulating IB dysfunction caused by HFD. Studies have found that HFD and overnutrition are critical initiating factors that may change intestinal flora,

lipid metabolism and systemic inflammation (3). HFD can reduce the expression of AGR2 and tight junction-related proteins in the colon, and increase colonic epithelial permeability, and AGR2 is negatively correlated with colonic permeability. This suggests that AGR2 may participate in maintaining intestinal barrier function (IBF) by upregulating tight junction proteins. Al Shaibi et al. (4) found that enteropathy caused by AGR2 deficiency, spherical cell loss and endoplasmic reticulum stress led to the defect of the mucous barrier and could not alleviate endoplasmic reticulum stress. And it could lead to inflammatory bowel disease in infancy, which in turn leads to abnormal intestinal mucosal barrier function. However, further research is needed on how the barrier function of animal models under HFD is affected by serum AGR2 levels. To verify this hypothesis, SD rats were fed with HFD for 8 weeks to establish a model. It detected serum and colon tissue

* Corresponding author. Email: shuhongzhao2022@163.com

AGR2 levels and evaluated changes in colon permeability. This study established an HFD rat model and observed the possible involvement of AGR2 in maintaining IBF by regulating tight junction proteins. This provided a new understanding of the effect of AGR2 on IB permeability and opened up new ideas for the treatment of metabolic-related intestinal diseases.

Materials and Methods

Experimental animals

30 healthy male clean-grade C57BL/6 mice were selected and purchased from Moulai Bao Biotechnology Co., Ltd. The age range is 6-7 weeks, with a body weight of 18-22g.

Methods

Main instruments and reagents

Scale: METTLER TOLEDO XS204 precision scale; Microplate reader: BioTek Synergy HTX multimode reader, produced by Boten Instruments Co., Ltd. in the United States; Protein blotting instrument and image analysis system: Bio-Rad ChemiDoc MP imaging system; Ussing chamber equipment: Physiological Instruments U2500 Ussing chamber system, including Ussing chamber, interlock compensator, ventilator and other equipment; Serum enzyme total cholesterol test kit, triglyceride enzyme test kit, double antibody sandwich ELISA AGR2 test kit, double antibody sandwich ELISA DAO test kit; Fully automatic biochemical analyzer (BK-600 model, Jinan Taiyi Biotechnology Co., Ltd.).

Preparation of the HFD model

Feeding conditions: The mice are raised in cages, providing them with free eating, drinking water, and pipeline activity space. The room temperature is controlled at $23 \pm 2^\circ\text{C}$, the relative humidity is 40% -60%, and the light cycle is 12 hours. They are fed a normal diet and distilled pure water to ensure the growth and development of mice. After one week of adaptive feeding, the experiment will be conducted. 30 mice are numbered and separated into a normal control group (NCG) and a high-fat group (HFG) of 15 each. The NCGs are fed a normal diet, while the HFGs are fed high-fat feed. The fat content in the high-fat feed is 20%, mainly from lard and soybean oil. Other nutritional components are similar to a normal diet. Normal diet: 184 g of casein, 156.8 g of wheat bran, 276 g of corn starch, 138 g of soybean flour, 55.2 g of vegetable oil, 32 g of vitamin mixture, 32 g of mineral mixture, 46 g of cellulose were prepared into 920 g of mixed feed; High-fat feed: 920g basic feed, 40g lard, 40g soybean oil, 2g cholesterol, and 10g cellulose. Feeding for a total of 8 weeks. Each mouse is raised in a single cage and can freely drink water. During the study period, weight monitoring will be conducted, and the weight of mice measured once a week to observe the trend of weight changes in both groups of mice.

Sample collection

Collection of serum samples: It collects samples using the mouse tail vein blood collection method. Blood collection steps: It selects healthy mice to check the tail vein blood vessels to ensure that they are visible. Fasting should

last for 12 hours before the examination. It needs to pull the hair out to expose the vein blood vessels after 75% alcohol disinfection and warm the tail of mice to make the tail vein congest. A 27G needle is put into the vein, and it connects a 1ml syringe to gently draw 0.3-0.5ml blood. After bleeding 0.1-0.2ml to relieve pressure, then blood extraction starts. After blood collection, it removes the needle and briefly compresses the needle hole to stop bleeding. It removes the syringe and immediately compresses the needle hole with a cotton ball for 30-60 seconds to stop bleeding. Let the whole blood stand for 1 hour, centrifuge for 10 minutes, at 3000 rpm, 4°C , and take the supernatant serum for backup.

Collection of intestinal tissue samples: After the collection of serum samples, 10% chloral is injected into the abdominal cavity at a weight of 0.3ml/100g, and the open site is disinfected. The abdomen is directly cut open, exposing the colon, jejunum, and related blood vessels. Approximately 4cm of the colon is removed from the proximal end of the spine, and approximately 8cm is removed from the distal end of the jejunum to remove fecal material. Exposed blood vessels are ligated or clamped to reduce bleeding within the tissue. The excised tissue is immediately placed in physiological saline and stored at 4°C to avoid tissue drying. It should be transported to the laboratory within 30 minutes. A circular incision should be made on the colon and the small intestine should be put into a sac. Then, the outer layer of the mucosa should be removed to facilitate drug penetration. Some tissues are preserved in liquid nitrogen for qPCR, while the rest are used for the Ussing chamber and EB detection. After tissue collection, the animals are euthanized and dissected to check for abnormalities in other organs. The process of collecting intestinal tissue specimens is carried out on ice.

Serological index examination

Serological samples were collected at the beginning of modeling (T0) and at 8 weeks of feeding (T1), and whole blood glucose, total cholesterol, and triglycerides were detected using enzymatic methods; ELISA is used to determine the concentration of AGR2 and DAO.

Intestinal tissue examination

It collects colon tissue from model rats and uses real-time fluorescence quantitative PCR to determine the expression of AGR2 mRNA in colon tissue. After extracting total RNA from colon tissue, it should be determined whether the quality and concentration meet the requirements, and then reverse transcription is performed. Synthesizing cDNA uses M-MLV reverse transcriptase. PCR primers and fluorescent probes are designed based on the AGR2 mRNA sequence. Primer sequence: upstream 5-GCC AGA AAA TGC TGG AGA AG-3; Downstream 5-AGG TCA TCC ACA GGC TCA TT-3. A qPCR reaction system is prepared according to the instructions of the kit, including primers, probes, and cDNA. It uses a real-time fluorescence quantitative PCR instrument for qPCR, the fluorescence signal is read to determine the Ct value. The $2^{-\Delta\Delta\text{Ct}}$ is used to work out the relative expression of AGR2. The expression changes of AGR2 mRNA in the HFG were obtained using the internal reference gene as internal reference and the control group as calibration. Each sample is set up with 3 multiple wells for qPCR, with Ct values within 0.5. The experiment is repeated 3 times.

Functional examination of IB

The colon of the mouse is cut into slices and the tissue is placed in two and a half of the ichiometric chambers in the Ussing chamber. Krebs Ringer solution with 95% oxygen -5% CO2 is perfused both internally and externaly, at 37 ° C and pH 7.4. After connecting the micro rotary injector and injecting glucose, glycine, or hydrochloric acid into the inner and outer chambers respectively, the changes in fluid flow in both chambers are recorded. It measures the short-circuit current value (Isc) and conductivity difference (Gt) using a current clamp, reflecting Na⁺permeability and epithelial tight junction integrity. Isc changes can reflect Na⁺ transport, while Gt changes can reflect epithelial permeability. The indicators are measured once every 15 minutes, and the experimental process lasts for 60-120 minutes. Summarizing, recording, and analyzing data by computer software Arcus Bio Purchase and Analysis instruments is to compare the mean values. After the experiment, the animals are euthanized and the sampling site is checked for bleeding or damage, as well as other factors that can affect the results.

It needs to prepare a small intestine sac by taking a section of small intestine tissue that has been cleaned and separated from fecal matter, approximately 7 cm long (leaving 1 cm long segments at each end of the excised jejunum, and suturing the remaining 5 cm jejunum with a loop of hanging thread to create an empty tubular structure). It injects 0.2ml of 1.5% EB solution into the intestinal sac in a 37 ° C water bath and opens the sac after 30 minutes, and rinses repeatedly with low-temperature PBS until the rinse solution is clear. After drying at 50 ° C for 24 hours, the dry mass of the intestinal sac is recorded. Formamide solution is added and incubated at 50 ° C for 24 hours. The supernatant is detected using a microplate reader and the optical density (OD) value at a wavelength of 650 nm is read. The content of Evan's blue (EB) in intestinal tissue is calculated based on the OD (650) value. The calculation expression is shown in Formula 1.

$$EB\ content(\mu g/g\ Stem\ tissue) = D \times 0.6 \times V/W \times 0.622 \times 10 \ [1]$$

In the formula: D represents the absorbance measured by the microplate reader, and a wavelength of 650nm is selected to read its absorbance value; V is the volume of EB solution, which is 0.2ml in this experiment; W is the dry weight of the organization.

Statistical processing

SPSS 26.0 software is applied for data statistics. Measurement data of normal distribution is represented in $\bar{x} \pm s$. Independent sample *t*-test is utilized for comparison with

hin groups, and paired sample *t*-test is adopted for comparison within groups at different time points. The test level is $\alpha= 0.05$. Pearson correlation analysis and scatter plots are used for correlation analysis.

Results

Modeling situation of two groups of mice

The body weight of the NCG and the HFG mice showed an upward trend, with the HFG having higher body weight at the 4th and 8th weeks, with a statistically significant difference ($P<0.05$) (Figure 1). From the changes in fasting blood glucose, total cholesterol, and triglycerides of mice, all indicators of the two groups of mice were higher than before the start of modeling after 8 weeks of feeding. However, the fasting blood glucose, total cholesterol, and triglycerides of the HFG mice were higher, and the difference had statistical significance ($P<0.05$) (Table 1). Both groups of mice were successfully modeled.

Comparison of serum AGR2 and DAO concentrations between two groups of mice

From the changes in serum AGR2 and DAO concentrations of mice, the serum AGR2 concentrations of the two groups of mice after 8 weeks of feeding were higher than before the start of modeling, but the AGR2 concentrations of the HFG mice were higher, with a statistically significant difference ($P<0.05$); When the mice in the two groups were fed for 8 weeks, there was no statistically significant difference in serum DAO concentration compared to before the start of modeling ($P>0.05$). The DAO concentration of the HFG mice was lower than the NCG, and the difference had statistical significance ($P<0.05$) (Table 2).

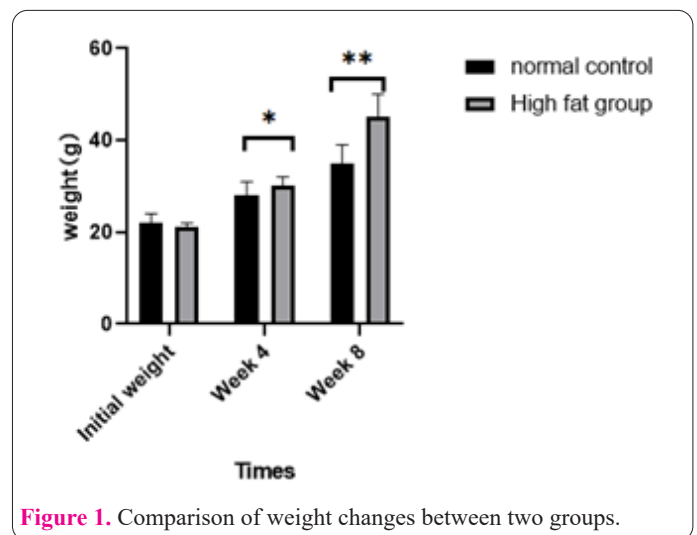


Figure 1. Comparison of weight changes between two groups.

Table 1. Comparison of serological indicators between two groups of mice ($\bar{x} \pm s$, mmol/L).

Group (n)	Fasting blood glucose		Total cholesterol		Triglyceride	
	T0	T1	T0	T1	T0	T1
NCG (15)	4.71±0.55	5.06±0.62	1.75±0.21	1.83±0.31	0.81±0.14	0.84±0.22
HFG (15)	4.69±0.64	5.67±0.82*	1.72±0.32	3.12±0.57*	0.88±0.24	1.70±0.5*
<i>t</i>	0.089	-2.331	0.215	-7.703	-0.851	-5.924
<i>P</i>	0.930	0.027	0.831	0.000	0.402	0.000

Note: T0 is before the start of modeling, and T1 is at 8 weeks of feeding. Compared with T0 in this group, * $P<0.05$.

Table 2. Comparison of serum AGR2 and DAO concentrations between two groups of mice.

Group (n)	Serum AGR2 (ng/mL)		DAO (U/mL)	
	T0	T1	T0	T1
NCG (15)	14.06±3.66	17.37±3.42*	13.46±2.55	12.42±3.18
HFG (15)	16.05±4.06	23.20±5.61 *	11.32±1.91	10.54±1.54
<i>t</i>	-1.412	-3.435	-2.584	2.057
<i>P</i>	0.169	0.002	0.169	0.049

Note: T0 is before the start of modeling, and T1 is at 8 weeks of feeding. Compared with T0 in this group, * *P*<0.05.

Table 3. Colon tissue AGR2 levels and intestinal permeability of two groups of mice.

Group (n)	AGR2 relative expression	Isc (μA/cm2)	Gt (mS/cm2)	EB content (μg/g)
NCG (15)	1.04±0.25	24.78±6.90	4.97±0.91	19.31±6.14
HFG (15)	1.66±0.41	10.89±2.02	7.93±1.94	31.66±8.77
<i>t</i>	-5.005	7.490	-5.335	-4.469
<i>P</i>	0.000	0.000	0.000	0.000

Table 4. Correlation of various indicators in HFD mice.

Indicators	Isc		Gt		EB content	
	<i>r</i>	<i>P</i>	<i>r</i>	<i>P</i>	<i>r</i>	<i>P</i>
Serum AGR2	-0.503	0.005	0.461	0.010	0.357	0.053
AGR2 relative expression	-0.623	0.000	0.560	0.001	0.177	0.350
Serum DAO	-0.264	0.158	0.485	0.007	0.437	0.016

AGR2 levels and intestinal permeability in colon tissue of two groups of mice

The relative expression levels of AGR2, Gt, and EB content in the colon tissue of the HFG mice were higher than those of the NCG, while Isc was lower than that of the NCG, with statistical significance (*P*<0.05) (Table 3).

Correlation of various indicators in HFD mice

The relative expression of serum AGR2 and colon AGR2 were negatively correlated with Isc (*r*=-0.503, -0.623, *P*<0.05), positively correlated with Gt (*r*=0.461, 0.560, *P*<0.05), and positively correlated with serum DAO and Gt, EB content (*r*=0.485, 0.437, *P*<0.05) (Table 4). From Figure 2, there was a homogeneous distribution characteristic between the relative expression of serum AGR2 and serum DAO, colon AGR2, and Isc variables.

Discussion

HFD can induce changes in microbial composition, thereby influencing intestinal immunity. Current evidence suggests a connection between gut microbiota and the production of uremic toxins, increased intestinal permeability, transmural movement of bacteria and endotoxins, and inflammation (5). HFD and lack of activity will result in increased inflammatory response, insulin resistance, oxidative and Nitrosation stress, and mitochondrial dysfunction (6). HFD is closely related to increased intestinal permeability and damage to barrier function, especially has important impacts on oxidative stress and inflammatory reaction. The characteristic of HFD-induced obesity is the chronic micro-inflammatory state of various tissues and organs. The colon is the first tissue organ to exhibit pro-inflammatory characteristics associated with changes in the gut microbiota (7). Therefore, the degree of damage to the colonic IBF is one of the indicators that clinical at-

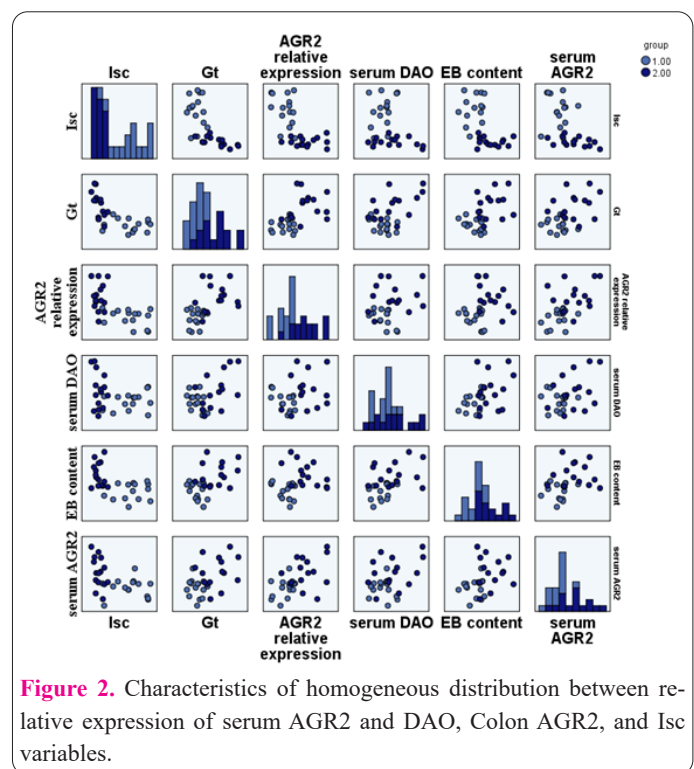


Figure 2. Characteristics of homogeneous distribution between relative expression of serum AGR2 and DAO, Colon AGR2, and Isc variables.

tention must be paid. The IB includes epithelial cells and indirect cellular complexes, which regulate epithelial ion transport and permeability (8). However, in the past, IBF can only be obtained through Ussing chamber technology (9). It requires the acquisition of intestinal epithelial cells, which is difficult to continuously and constantly monitor, and belongs to traumatic monitoring. These deficiencies will inevitably affect the evaluation of the patient's IBF.

AGR2 protein is secreted in both human and rat mammalian epithelial cells (10). The overexpression of AGR2 is related to bad prognosis in digestive system cancer.

AGR2 participates in the homeostasis of epithelial cells and is secreted in both the small and large intestine (11). Boisteau et al. (12) found that the deletion of the AGR2 gene protein led to severe intestinal inflammation. Even in inflammatory bowel disease, the secretion of AGR2 in the extracellular environment participated in the remodeling of the cell microenvironment (13). At the same time, the loss of AGR2 gene expression also led to the attenuation of terminally differentiated cells, which were replaced by SOX9-labeled cells. The absence of AGR2 and the expression of Sox9 are both related to progenitor cells and stem cells, and both have similar effects on intestinal cell proliferation (14). AGR2 affects intestinal homeostasis and endoplasmic reticulum stress (15,16). AGR2 can maintain a balance between proliferative and differentiated epithelial cells. Under the induction of HFD, intestinal epithelial cells exhibit insulin resistance and increased oxidative stress, while utilizing redox regulatory mechanisms can partially alleviate pathological changes (14,17). Therefore, as a dynamic monitoring method, the serum concentration of AGR2 can make up for the deficiencies in the current detection of IBF.

It was proved that when the two groups of mice were fed for 8 weeks, their body weight, fasting blood glucose, total cholesterol, and triglycerides all met the modeling characteristics of HFD mice, and the modeling was successful. Persistent HFD caused intestinal microbiota imbalance, increased cell apoptosis, decreased expression of intercellular connections and epithelial tight junction proteins, decreased intestinal secretion and mucus secretion, and other changes in mice, leading to damage to the structure and function of the IB, followed by weight gain, elevated blood sugar and lipid levels. Further monitoring of serum AGR2 concentration and DAO concentration in this study revealed that HFD caused an increase in serum AGR2 concentration and a decrease in DAO concentration in mice. This result was related to the involvement of AGR2 in the MLCK/p-MLC pathway (18). DAO was mainly used as the main amino oxidase in small intestinal epithelial cells, and its activity could be used as a biochemical indicator to determine small IBF (19). From the results, in the HFD mouse model, serum AGR2 and DAO could be used as indicators for evaluating IBF. In addition, the relative expression level of AGR2 in mouse colon tissue was similar to the changes in serum AGR2 concentration. AGR2 could also reflect the IBF of colon tissue.

The outcomes of this study expressed that AGR2 might act as a potential biomarker for oxidative stress and epithelial cell damage, closely related to evaluating changes in IBF, and could provide new ideas for the treatment and intervention of IB dysfunction. The relative expression of serum AGR2 and colon AGR2 were negatively correlated with Isc ($r=-0.503$, -0.623 , $P<0.05$), positively correlated with Gt ($r=0.461$, 0.560 , $P<0.05$), and positively correlated with serum DAO and Gt, EB content ($r=0.485$, 0.437 , $P<0.05$). There was a homogeneous distribution characteristic between the relative expression of serum AGR2 and serum DAO, colon AGR2, and Isc variables. However, the new role of AGR2 in liver and intestinal fatty acid uptake and activation promoted AGR2-mediated lipid accumulation, indicating that AGR2 was an important regulator of systemic lipid metabolism, and downregulation of AGR2 might counteract the development of obesity (20). The IBF depended on intestinal permeability (21). This study

evaluated the Isc, Gt, and EB contents of colon and small intestine tissues respectively, which could form a more comprehensive evaluation advantage. From the outcomes, it has no significant correlation between AGR2 and EB content in small intestine tissue. In the future, AGR2 combined with DAO can be used to further clarify the damaged areas of IBF.

In summary, this study preliminarily confirms that AGR2 may participate in the regulation of IBF caused by HFD. Its changes can serve as potential biomarkers for evaluating IB damage, providing a theoretical basis for the pathogenesis and treatment of IB dysfunction. However, the specific mechanism of AGR2 in this pathological process needs further experimental research to confirm. In the future, with the deepening of research, it is expected to discover that AGR2 is the main factor, providing new ideas for the study of the pathogenesis and treatment targets of metabolic-related intestinal diseases.

Fundings

The research is supported by: Zhoushan municipal public welfare science and technology projects, (Rural and Social Development Science and Technology Division), Study on the Mechanism of Intestinal Mucosal Barrier Damage Aggravating Liver Lipidosis, (NO. 2020C33057).

References

1. Riedel S, Pheiffer C, Johnson R, Louw J, Muller CJF. Intestinal Barrier Function and Immune Homeostasis Are Missing Links in Obesity and Type 2 Diabetes Development. *Front Endocrinol (Lausanne)* 2022; 12: 833544. <https://doi.org/10.3389/fendo.2021.833544>
2. Ye X, Wu J, Li J, Wang H. Anterior Gradient Protein 2 Promotes Mucosal Repair in Pediatric Ulcerative Colitis. *Biomed Res Int* 2021; 2021: 6483860. <https://doi.org/10.1155/2021/6483860>
3. Guo Z, Ali Q, Abaidullah M, Gao Z, Diao X, Liu B, Wang Z, Zhu X, Cui Y, Li D, Shi Y. High fat diet-induced hyperlipidemia and tissue steatosis in rabbits through modulating ileal microbiota. *Appl Microbiol Biotechnol* 2022; 106(21): 7187-7207. <https://doi.org/10.1007/s00253-022-12203-7>
4. Al-Shaibi AA, Abdel-Motal UM, Hubrack SZ, Bullock AN, Al-Marri AA, Agrebi N, Al-Subaiey AA, Ibrahim NA, Charles AK; COLORS in IBD-Qatar Study Group; Elawad M, Uhlig HH, Lo B. Human AGR2 Deficiency Causes Mucus Barrier Dysfunction and Infantile Inflammatory Bowel Disease. *Cell Mol Gastroenterol Hepatol* 2021; 12(5): 1809-1830. <https://doi.org/10.1016/j.jcmgh.2021.07.001>
5. Cooper TE, Scholes-Robertson N, Craig JC, Hawley CM, Howell M, Johnson DW, Teixeira-Pinto A, Jaure A, Wong G. Synbiotics, prebiotics and probiotics for solid organ transplant recipients. *Cochrane Database Syst Rev* 2022; 9(9): CD014804. <https://doi.org/10.1002/14651858.CD014804.pub2>
6. Slyepchenko A, Maes M, Machado-Vieira R, Anderson G, Solmi M, Sanz Y, Berk M, Köhler CA, Carvalho AF. Intestinal Dysbiosis, Gut Hyperpermeability and Bacterial Translocation: Missing Links Between Depression, Obesity and Type 2 Diabetes. *Curr Pharm Des* 2016; 22(40): 6087-6106. <https://doi.org/10.2174/1381612822666160922165706>
7. Cao C, Tan X, Yan H, Shen Q, Hua R, Shao Y, Yao Q. Sleeve gastrectomy decreases high-fat diet induced colonic pro-inflammatory status through the gut microbiota alterations. *Front Endocrinol (Lausanne)* 2023; 14: 1091040. <https://doi.org/10.3389/fendo.2023.1091040>

8. Feng XY, Zhang DN, Wang YA, Fan RF, Hong F, Zhang Y, Li Y, Zhu JX. Dopamine enhances duodenal epithelial permeability via the dopamine D₅ receptor in rodent. *Acta Physiol (Oxf)* 2017; 220(1): 113-123. <https://doi.org/10.1111/apha.12806>
9. Rao YX, Chen J, Chen LL, Gu WZ, Shu XL. [Changes in tight junction protein expression and permeability of colon mucosa in rats with dextran sulfate sodium-induced inflammatory bowel disease]. *Zhongguo Dang Dai Er Ke Za Zhi* 2012; 14(12): 976-981. Chinese.
10. Clarke C, Rudland P, Barraclough R. The metastasis-inducing protein AGR2 is O-glycosylated upon secretion from mammary epithelial cells. *Mol Cell Biochem* 2015; 408(1-2): 245-252. <https://doi.org/10.1007/s11010-015-2502-3>
11. Pelaseyed T, Bergström JH, Gustafsson JK, Ermund A, Birchenough GM, Schütte A, van der Post S, Svensson F, Rodríguez-Piñeiro AM, Nyström EE, Wising C, Johansson ME, Hansson GC. The mucus and mucins of the goblet cells and enterocytes provide the first defense line of the gastrointestinal tract and interact with the immune system. *Immunol Rev* 2014; 260(1): 8-20. <https://doi.org/10.1111/imr.12182>
12. Boisteau E, Posseme C, Di Modugno F, Edeline J, Coulouarn C, Hrstka R, Martisova A, Delom F, Treton X, Eriksson LA, Chevet E, Lièvre A, Ogier-Denis E. Anterior gradient proteins in gastrointestinal cancers: from cell biology to pathophysiology. *Oncogene* 2022; 41(42): 4673-4685. <https://doi.org/10.1038/s41388-022-02452-1>
13. Zhao F, Edwards R, Dizon D, Afrasiabi K, Mastroianni JR, Geyfman M, Ouellette AJ, Andersen B, Lipkin SM. Disruption of Paneth and goblet cell homeostasis and increased endoplasmic reticulum stress in *Agr2*^{-/-} mice. *Dev Biol* 2010; 338(2): 270-279. <https://doi.org/10.1016/j.ydbio.2009.12.008>
14. Gupta A, Wodziak D, Tun M, Bouley DM, Lowe AW. Loss of anterior gradient 2 (*Agr2*) expression results in hyperplasia and defective lineage maturation in the murine stomach. *J Biol Chem* 2013; 288(6): 4321-4333. <https://doi.org/10.1074/jbc.M112.433086>
15. Park SW, Zhen G, Verhaeghe C, Nakagami Y, Nguyen LT, Barczak AJ, Killeen N, Erle DJ. The protein disulfide isomerase AGR2 is essential for production of intestinal mucus. *Proc Natl Acad Sci U S A* 2009; 106(17): 6950-6955. <https://doi.org/10.1073/pnas.0808722106>
16. Bergström JH, Berg KA, Rodríguez-Piñeiro AM, Stecher B, Johansson ME, Hansson GC. AGR2, an endoplasmic reticulum protein, is secreted into the gastrointestinal mucus. *PLoS One* 2014; 9(8): e104186. <https://doi.org/10.1371/journal.pone.0104186>
17. Cremonini E, Daveri E, Mastaloudis A, Adamo AM, Mills D, Kalanetra K, Hester SN, Wood SM, Fraga CG, Oteiza PI. Anthocyanins protect the gastrointestinal tract from high fat diet-induced alterations in redox signaling, barrier integrity and dysbiosis. *Redox Biol* 2019; 26: 101269. <https://doi.org/10.1016/j.redox.2019.101269>
18. Ye X, Sun M. AGR2 ameliorates tumor necrosis factor- α -induced epithelial barrier dysfunction via suppression of NF- κ B p65-mediated MLCK/p-MLC pathway activation. *Int J Mol Med* 2017; 39(5): 1206-1214. <https://doi.org/10.3892/ijmm.2017.2928>
19. Ono M, Ishii A, Aritsune M, Horikita T. Changes in serum concentration and activity of diamine oxidase during the first month of life in calves. *J Vet Med Sci* 2023; 85(4): 417-419. <https://doi.org/10.1292/jvms.22-0343>
20. Wang Y, Jia M, Liang C, Sheng N, Wang X, Wang F, Luo Y, Jiang J, Cai L, Niu H, Zhu D, Nesa EU, Young CY, Yuan H. Anterior gradient 2 increases long-chain fatty acid uptake via stabilizing FABP1 and facilitates lipid accumulation. *Int J Biol Sci* 2021; 17(3): 834-847. <https://doi.org/10.7150/ijbs.57099>
21. Wang B, An N, Shaikh AS, Wang H, Xiao L, Liu H, Li J, Zhao D. Hyperosmolarity evokes histamine release from ileum mucosa by stimulating a cholinergic pathway. *Biochem Biophys Res Commun* 2017; 493(2): 1037-1042. <https://doi.org/10.1016/j.bbrc.2017.09.093>